

Fluid substitution with Dynamic Fluid Modulus: facing the challenges in heterogeneous rocks

Qiuliang Yao*, De-Hua Han, Fuyong Yan, Luanxiao Zhao, Rock Physics Lab, University of Houston

Summary

A new concept of frequency dependent effective fluid modulus is proposed to characterize the velocity dispersion caused by wave induced fluid flow (WIFF). It has a clear physical meaning and simple math expression, and can be directly used in Gassmann equation to predict the dispersion and attenuation. The new method is applied to a pore-crack system to predict squirt flow dispersion, either with single or multiple sets of cracks. Inverting the effective fluid modulus from measured ultrasonic data provides an indicator of the heterogeneity of the rock.

Introduction

By allowing the relative movement between solid frame and fluid, Biot (1956a, 1956b, 1962) first revealed wave induced fluid flow and the dispersion/attenuation associated with it. Since then, many more WIFF related dispersion/attenuation mechanisms have been proposed and formulated. Squirt flow models (O'Connell and Budiansky, 1977; Dvorkin *et al.*, 1995) focus on the fluid flow from softer cracks to stiffer round pores at grain scale. White (1975) studied fluid flow caused by compressibility heterogeneity between two immiscible fluids (patch saturation). Double porosity and dual permeability model (Berryman and Wang 1995; Pride and Berryman 2003a, 2003b) provides a general framework to explicitly relate the internal fluid flow to bulk modulus dispersion, and can cover mesoscopic heterogeneities which are recently believed to account for the majority of the dispersion and attenuation observed in seismic frequency range. In their approach, many rock parameters, including drained and undrained bulk moduli, and Skempton's coefficient, have been formulated as frequency dependent effective properties. We're here seeking an alternative approach to use only one frequency dependent effective property: fluid modulus, which is directly related to the fluid flow, to model the non-Biot dispersion.

Partial drainage and effective fluid modulus

Gassmann equation predicts the fluid effect under undrained condition. "Undrained" means the boundary is closed so that no fluid allowed to flow into or out from a representative element volume (REV). What happens if the boundary is not fully closed? It has been experimentally observed that bulk modulus drops if there is leak at the surface of the core sample (Hofmann, 2006). If part of the pore fluid is squeezed out of the REV, then the extra support by the fluid will be decreased. If there is additional fluid flowing into the REV, then the extra support is increased. We can introduce an "effective fluid modulus"

to account for this partial drainage effect. A decreased support can be equivalent to a "still closed system but with reduced fluid modulus", and vice versa, an increased support can be modeled as an increased fluid modulus. (Figure 1)

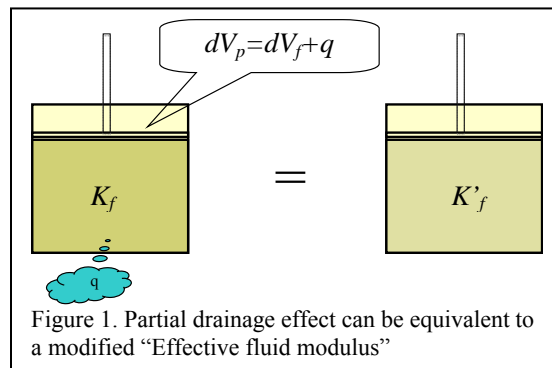


Figure 1. Partial drainage effect can be equivalent to a modified "Effective fluid modulus"

At closed undrained condition, the pore volume change equals to fluid volume change, so that we can write

$$\frac{dV_p/V_p}{dP_p} = \frac{dV_f/V_f}{dP_f} = -\frac{1}{K_f} \quad (1)$$

At partial drained condition, the pore volume change equals to the fluid volume change plus the flow amount q . We define the incoming flow as positive and outgoing flow as negative value. Note that under increasing external pressure, the pore volume change is negative. If one defines an effective fluid modulus K'_f to correspond to the modified fluid volume change:

$$\frac{1}{K'_f} = -\frac{(dV_p + q)/V_p}{dP_p} = -\frac{1}{K_f} - \frac{q/V_p}{dP_p} \quad (2)$$

Then one can still use Gassmann with this K'_f , since the partial drainage effect is equivalently included in this modified fluid modulus.

$$K_{sat} = K_{dry} + \frac{\alpha^2}{(\alpha - \phi)/K_0 + \phi/K'_f} \quad (3)$$

Internal fluid flow and bulk compressibility

Next, we move on to consider the internal fluid flow caused by rock frame heterogeneity. In this case, the flow does not occur at the outer surface of the REV, but between the different parts of the rock within the REV. Part of the rock has an income flow and the other part

Dynamic Fluid Modulus

has an outgoing flow. There is a coupling between the incoming and outgoing flows. Actually this provides a constraint that we can use to compute the q .

First we present a derivation of the maximum q , which represents the fluid flow amount at zero frequency.

Consider a REV consisting of two type of pores with pore volume V_{p1} and V_{p2} respectively. Type 1 is stiffer with bulk modulus K_{dry1} and type 2 is softer with bulk modulus K_{dry2} (Figure 2). Assuming under iso-stress condition a positive external pressure is applied to the REV, so that both types of pores receive the same confining pressure P_c .

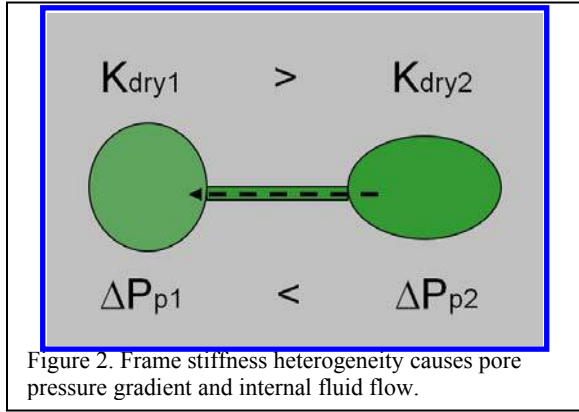


Figure 2. Frame stiffness heterogeneity causes pore pressure gradient and internal fluid flow.

First, at the high frequency end, each type of pore is under undrained condition so that the pore pressure increases separately depending only on its own frame properties.

$$K_f = -\frac{dP_{p1}}{dV_{p1}/V_{p1}} = -\frac{dP_{p2}}{dV_{p2}/V_{p2}} \quad (4)$$

Here the pore pressure increment in each phase is related to the corresponding confining pressure change dP_c by (Thomsen, 1985; Skempton, 1954):

$$dP_p = \frac{\alpha K_f}{K_d \left[\phi + \frac{K_f}{K_0} (\alpha - \phi) + \alpha^2 K_f \right]} dP_c \quad (5)$$

Now at zero frequency, fluid in amount of q flows from pore type 2 to pore type 1, so in pore type 1, we have

$$dP_{p1}' = -K_f \frac{dV_{p1} - q}{V_{p1}} \quad (6)$$

And for pore type 2 we have

$$dP_{p2}' = -K_f \frac{dV_{p2} + q}{V_{p2}} \quad (7)$$

Since they are equilibrated, $dP_{p1}' = dP_{p2}'$. Combining (4), we can obtain:

$$q = \frac{1}{K_f} \frac{dP_{p2} - dP_{p1}}{1/V_{p1} + 1/V_{p2}} \quad (8)$$

When $V_{p1} \gg V_{p2}$, (8) can be approximated as

$$q = \frac{V_{p2}}{K_f} (dP_{p2} - dP_{p1}) \quad (9)$$

Next, we will show how this fluid flow amount q can be related to the change of bulk compressibility of the rock. For better clarity, here we use the notation of fluid compressibility instead of modulus in our derivation.

At high frequency, there is no fluid exchange between any pores. Each type of pore just behave as a completely closed system, the pore volume changes in type 1 and type 2 are

$$\delta V_1 = -\beta_f V_1 \delta P_{p1} \quad (10)$$

$$\delta V_2 = -\beta_f V_2 \delta P_{p2} \quad (11)$$

So the total volume change is

$$\delta V_H = \delta V_1 + \delta V_2 = -\beta_f (V_1 \delta P_{p1} + V_2 \delta P_{p2}) \quad (12)$$

Then we consider at low frequency (0Hz), there is q amount of fluid moved from V_2 into V_1 , so we can write:

$$\delta V_1' = -\beta_f (V_1 + q) \delta P_p \quad (13)$$

$$\delta V_2' = -\beta_f (V_2 - q) \delta P_p \quad (14)$$

And the total volume change is

$$\delta V_L = \delta V_1' + \delta V_2' = -\beta_f (V_1 + V_2) \delta P_p \quad (15)$$

Now let us look at the difference of the total volume change between low frequency and high frequency cases:

$$\delta V_L - \delta V_H = -\beta_f [V_1 (\delta P_p - \delta P_{p1}) + V_2 (\delta P_p - \delta P_{p2})] \quad (16)$$

When $V_1 \gg V_2$, the fluid flow will barely change the pore pressure in V_1 thus we have the first term in right hand side vanished, and (16) can be approximated to:

$$\delta V_L - \delta V_H = -\beta_f V_2 (\delta P_p - \delta P_{p2}) \quad (17)$$

Compared to (9), this is just the amount of fluid moved from V_2 into V_1 . So we can conclude that under the condition that soft space is much smaller than stiff space, the same applied stress will cause a larger deformation at zero frequency than at high frequency due to the fluid flow from soft space into stiff space. The difference between them is approximately equal to the volume of the fluid flow from the soft space to stiff space.

In this sense, we can view the zero frequency case as a partial drained condition from high frequency end. However, if we want to build the dispersion curve above

Dynamic Fluid Modulus

the well established Gassmann formulation which represent the zero frequency, we should treat it in a reversed way, that any non-zero frequency case is a partial drained condition based on zero frequency point, with an incoming flow in the amount of $q' = (q_{max} - q)$. Here q_{max} is defined by (8), or can be obtained from any specific modeling by set frequency $f=0$ Hz (Figure 3). Based on this analysis, we can modify (2) to the following:

$$\frac{1}{K_f''} = \frac{1}{K_f} - \frac{q'/V_p}{dP_p} \quad (18)$$

Now, for any non-zero frequency, we can just simply use the frequency dependent $1/K_f'$ to replace the original $1/K_f$ in Gassmann equation, to fully and correctly characterize the velocity dispersion and attenuation.

$$K_{sat} = K_{dry} + \frac{\alpha^2}{(\alpha - \phi)/K_0 + \phi/K_f''} \quad (19)$$

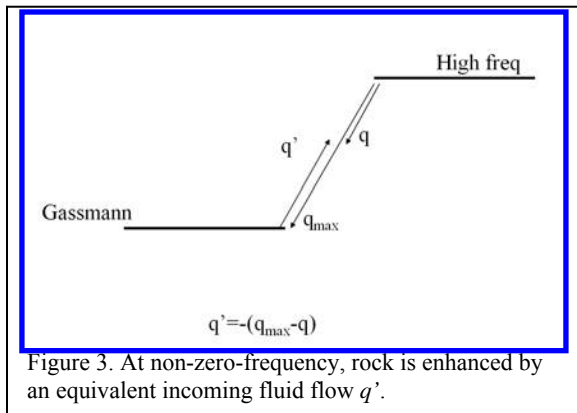


Figure 3. At non-zero-frequency, rock is enhanced by an equivalent incoming fluid flow q' .

Example: Squirt flow in pore-crack system

So the problem left with us now is to find out the amount of fluid flow q . Obviously, this q should be associated with the following factors: pressure gradient at boundary, local permeability at boundary, and fluid viscosity. Those in turns should be functions of frequency. Derivation of analytical expression of fluid flow q requires detailed information on the geometry of the heterogeneity. It normally involves Navier-Stokes equation with some assumption on the boundary conditions. Certain approximations are also required to obtain practical solutions. Nevertheless, due to the nature that all internal flows are diffusive like flows, it is possible to use a general format on internal fluid flow (Berryman, 2003):

$$q = \frac{q_{max}}{(1 - iP\omega/\omega_c)^{1/2} - i\omega/\omega_c} \quad (20)$$

One special case for round pore plus thin cracks is described and formulated by Tang (2011).

$$\frac{q}{\partial P_f V_f} = \frac{8\pi\epsilon(1-\nu)}{3\phi\mu} f(\zeta) \left[\frac{1/K_f' - 1/K_f}{1/K_f' - 1/K} - f(\zeta) \right] \left/ \left[1 + \frac{4(1-\nu)K_f}{3\mu\gamma} [1 - f(\zeta)] \right] \right. \quad (21)$$

The two dominant controlling parameters are crack density ϵ and crack aspect ratio γ . We use this expression of q to model the P wave dispersion in a crack-pore system (Figure 4b). All input rock and fluid parameters are the same as in Tang (2011). Compared to Tang's original results (Figure 4a), our results predict all non-zero-frequency velocities above the Gassmann value, due to the additional step of $q' = q_{max} - q$ discussed before.

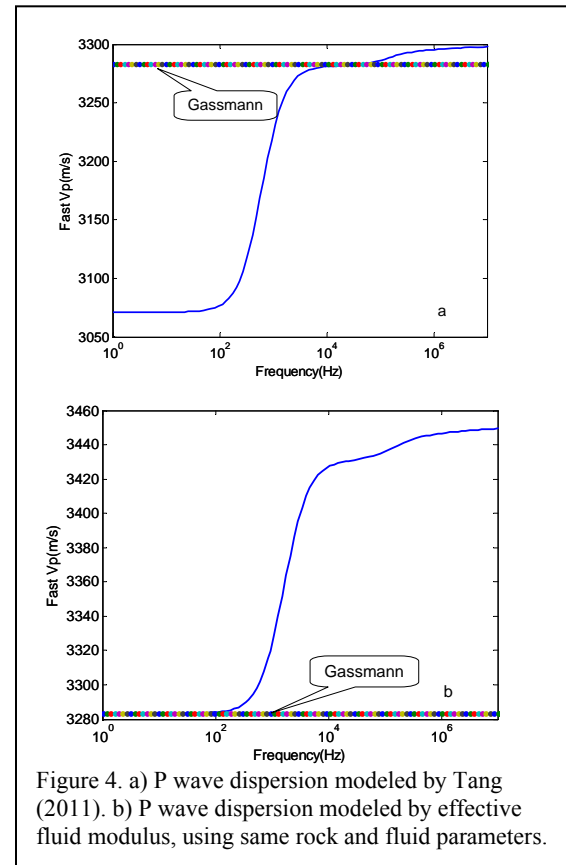


Figure 4. a) P wave dispersion modeled by Tang (2011). b) P wave dispersion modeled by effective fluid modulus, using same rock and fluid parameters.

Although we use the name "effective fluid modulus" to account for the dispersion and attenuation associated with WIFF (wave induced fluid flow), it must be point out that it is just an equivalent concept, and the dispersion and attenuation are actually not caused by changing property of the fluid. It is rather caused by the heterogeneity. This heterogeneity can either be on the solid frame (like crack-pore model or double porosity model), or on the fluid (patchy model). We can think the effective fluid modulus as an indicator of the heterogeneity.

Furthermore, in real rock, multiple scales of heterogeneities can coexist either in discrete or

continuous spectrum. If each set of heterogeneity can be represented by a corresponding effective fluid modulus, then the total heterogeneity can be represented by

$$\frac{1}{K_f'} = \frac{1}{K_f} - \sum_i \frac{q_i' / V_p}{dP_p} \quad (22)$$

With this concept, in Figure 5, we simulate a rock with 7 sets of cracks. Panel a shows the crack density and aspect ratio for each set of crack. In panel b we display both the real (red) and imaginary (blue) parts of the overall effective fluid modulus, along with the original fluid modulus of 2.25GPa, which represents the homogeneous rock. The multiple scales of heterogeneities in this simulation predict a wide spectrum of fast P-wave velocity dispersion and attenuation, which are often observed in real reservoir rocks (c and d).

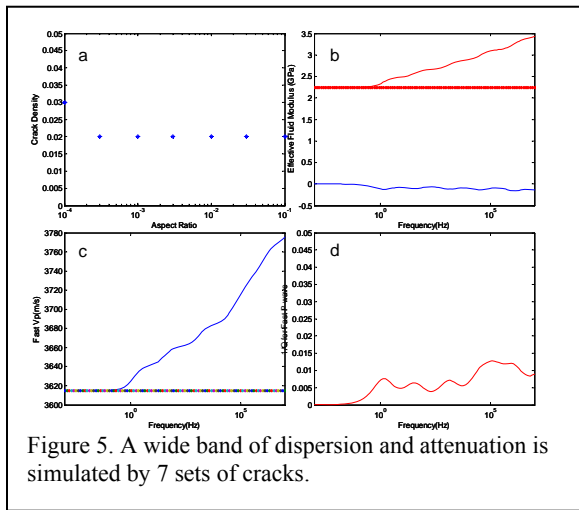


Figure 5. A wide band of dispersion and attenuation is simulated by 7 sets of cracks.

Invert K_f' from ultrasonic data

While broad band laboratory measurement data are still rarely available, we can use widely available ultrasonic data to invert the effective fluid moduli at the particular measurement frequency, and use them as indicators of heterogeneity, to get some insights to the composition, structure, and texture of the interested rock.

In Figure 6, we use a subset of Han’s data (Han, 1986) to calculate the real part of the effective fluid moduli at differential pressure range of 5-50MPa. While an original value of 2.25GPa represents the no heterogeneity and no wave induced fluid flow, we can see all samples exhibit certain level of heterogeneity and the ultrasonic wave can generate certain amount of internal fluid flow within the sample. Increasing the differential pressure may slightly reduce the heterogeneity for most of the samples, especially for the two samples that has much large heterogeneity compared with the rest of the group. Better interpretation could be expected, should the effective fluid modulus data

be analyzed together with other information, like porosity, permeability, cementation, and thin section images.

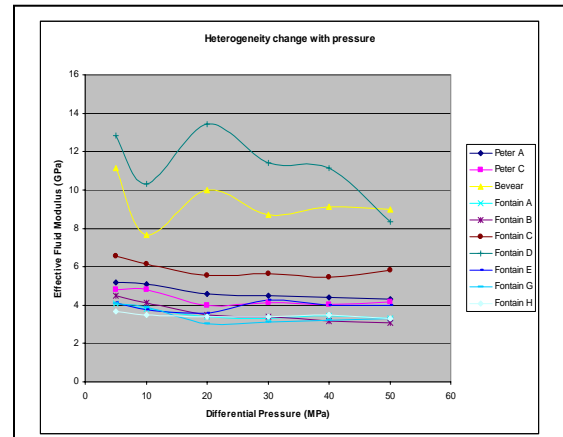


Figure 6. Effective fluid moduli inverted from ultrasonic measurement data indicate the rock heterogeneities and response to pressure change.

Discussion

The most important equation in the context is equation (18), which can also be written in the form of compressibility rather than bulk modulus:

$$\beta' = \beta - \frac{q' / V_p}{dP_p} \quad (23)$$

Obviously the second term can be viewed as a modification to the compressibility of the virgin pore fluid, caused by the internal fluid flow across a boundary separating the different phases inside a REV. It has the same dimension as the compressibility. The appearance of dP_p seems making the whole term with an experiment parameter dependency. However, in the small strain linear domain, the fluid flow amount q' is always proportional to the applied pressure dP_c and the induced pore pressure increment dP_p , therefore in any final analytical expression of the effective fluid compressibility, the dP_p will not appear.

Conclusion

Through poroelasticity analysis, we suggest to use an effective fluid modulus to link the bulk modulus dispersion to internal fluid flow, so that Gassmann fluid substitution is extended into non-homogeneous rock at none zero frequencies. It is successfully applied to predict squirt flow dispersion. Multiple heterogeneities can be easily handled with the new method as demonstrated in our example.

Downloaded 10/18/13 to 129.7.247.234. Redistribution subject to SEG license or copyright; see Terms of Use at http://library.seg.org/

<http://dx.doi.org/10.1190/segam2013-1226.1>

EDITED REFERENCES

Note: This reference list is a copy-edited version of the reference list submitted by the author. Reference lists for the 2013 SEG Technical Program Expanded Abstracts have been copy edited so that references provided with the online metadata for each paper will achieve a high degree of linking to cited sources that appear on the Web.

REFERENCES

- Berryman, J. G., and H. F. Wang, 1995, The elastic coefficients of double-porosity models for fluid transport in jointed rock: *Journal of Geophysical Research*, **100**, B12, 24,611–24,627, <http://dx.doi.org/10.1029/95JB02161>.
- Biot, M. A., 1956a, Theory of propagation of elastic waves in fluid-saturated porous solid: I, Low-frequency range: *The Journal of the Acoustical Society of America*, **28**, no. 2, 168–178, <http://dx.doi.org/10.1121/1.1908239>.
- Biot, M. A., 1956b, Theory of propagation of elastic waves in a fluid-saturated porous solid: II, Higher frequency range: *The Journal of the Acoustical Society of America*, **28**, no. 2, 179–191, <http://dx.doi.org/10.1121/1.1908241>.
- Biot, M. A., 1962, Mechanics of deformation and acoustic propagation in porous media: *Journal of Applied Physics*, **33**, no. 4, 1482–1498, <http://dx.doi.org/10.1063/1.1728759>.
- Dvorkin, J., G. Mavko, and A. Nur, 1995, Squirt flow in fully saturated rocks: *Geophysics*, **60**, 97–107, <http://dx.doi.org/10.1190/1.1443767>.
- Han, D., 1986, Effects of porosity and clay content on acoustic properties of sandstones and unconsolidated sediments: Ph.D. dissertation, Stanford University.
- Hofmann, R., 2006, Frequency dependent elastic and anelastic properties of clastic rocks: Ph.D. dissertation, Colorado School of Mines.
- O'Connell, R. J., and B. Budiansky, 1977, Viscoelastic properties of fluid-saturated cracked solids: *Journal of Geophysical Research*, **82**, no. 36, 5719–5735, <http://dx.doi.org/10.1029/JB082i036p05719>.
- Pride, S. R., and J. G. Berryman, 2003a, Linear dynamics of double-porosity dual-permeability materials: I, Governing equations and acoustic attenuation: *Physical Review E: Statistical, Nonlinear, and Soft Matter Physics*, **68**, no. 3, 036603, <http://dx.doi.org/10.1103/PhysRevE.68.036603>.
- Pride, S., and J. Berryman, 2003b, Linear dynamics of double-porosity and dual permeability materials: II, Fluid transport equations: *Physical Review E: Statistical, Nonlinear, and Soft Matter Physics*, **68**, no. 3, 036604, <http://dx.doi.org/10.1103/PhysRevE.68.036604>.
- Skempton, A. W., 1954, The pore-pressure coefficients A and B: *Geotechnique*, **4**, no. 4, 143–147, <http://dx.doi.org/10.1680/geot.1954.4.4.143>.
- Tang, X., 2011, A unified theory for elastic wave propagation through porous media containing cracks — An extension of Biot's poroelastic wave theory: *Science China: Earth Science*, **54**, 1441–1452.
- Thomsen, L., 1985, Biot-consistent elastic moduli of porous rocks: Low-frequency limit: *Geophysics*, **50**, 2797–2807, <http://dx.doi.org/10.1190/1.1441900>.
- White, J. E., 1975, Computed seismic speeds and attenuation in rocks with partial gas saturation: *Geophysics*, **40**, 224–232, <http://dx.doi.org/10.1190/1.1440520>.